



HAL
open science

Evaluation of the effect of Tetramethylammonium hydroxide on the corrosion inhibition of A9M steel in industrial water an experimental, morphological and MD simulation insights.

K. Abderrahim, T. Chouchane, I. Selatnia, A. Sid, Paul Mosset

► To cite this version:

K. Abderrahim, T. Chouchane, I. Selatnia, A. Sid, Paul Mosset. Evaluation of the effect of Tetramethylammonium hydroxide on the corrosion inhibition of A9M steel in industrial water an experimental, morphological and MD simulation insights.. Chemical Data Collections, 2020, 28, pp.100391. 10.1016/j.cdc.2020.100391 . hal-02864511

HAL Id: hal-02864511

<https://univ-rennes.hal.science/hal-02864511v1>

Submitted on 15 Jun 2020

HAL is a multi-disciplinary open access archive for the deposit and dissemination of scientific research documents, whether they are published or not. The documents may come from teaching and research institutions in France or abroad, or from public or private research centers.

L'archive ouverte pluridisciplinaire **HAL**, est destinée au dépôt et à la diffusion de documents scientifiques de niveau recherche, publiés ou non, émanant des établissements d'enseignement et de recherche français ou étrangers, des laboratoires publics ou privés.

Chemical Data Collections article template

Title: Evaluation of the effect of Tetramethylammonium hydroxide on the corrosion inhibition of A9M steel in industrial water: an experimental, morphological and MD simulation insights.

Authors: K. Abderrahim¹, T.Chouchane², I. Selatnia^{3*}, A. Sid³ and P. Mosset⁴

Affiliations: ¹Surface Engineering Laboratory (L.I.S), Badji Mokhtar University, B.P.12-23000, Annaba, Algeria.

²Research Center In industrial Technology CRTI, P.O.Box 64, Cheraga 16014 Algiers, Algeria.

³Laboratory of Analytical Sciences, Materials and Environmental (LSAME). Larbi Ben M'Hidi University. Oum El Bouaghi. 04000. Algeria.

⁴Université de Rennes 1, Institut des Sciences Chimiques de Rennes, CNRS UMR 6226, Avenue du Général Leclerc, 35042 Rennes Cedex, France.

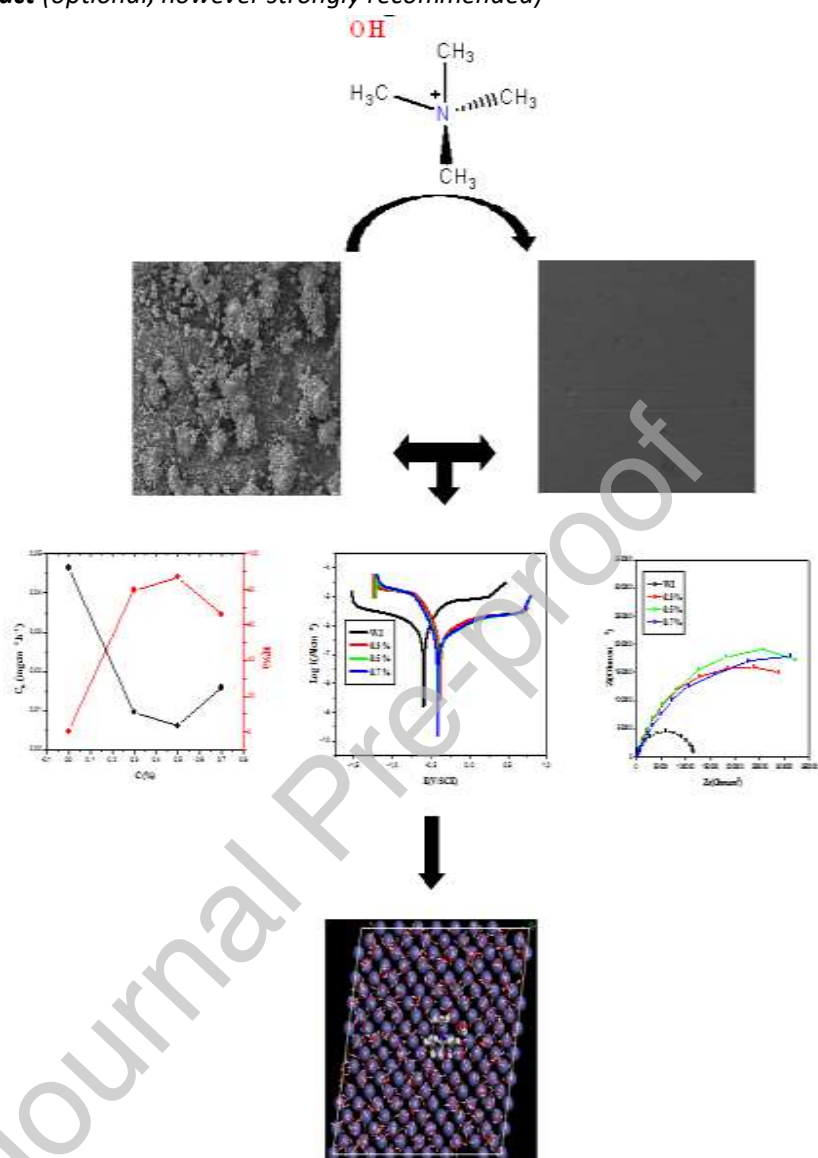
Contact email: ilhem.k2006@gmail.com

Abstract

Corrosion inhibition performance of Tetramethylammonium hydroxide (TMAH), for A9M steel in industrial water (IW) was investigated using weight loss, potentiodynamic polarization and EIS measurement. The results showed that the inhibition efficiency of the TMAH increases with the increase of its concentration which acts as anodic inhibitor. The Characterizations that have been performed as the surface morphology by optical microscope, surface roughness and scanning electron microscopy (SEM) have proved that TMAH can exhibit good inhibition ability by forming a protective film on A9M steel surface. Molecular dynamics simulation were used to investigate the strength of the interactions between metal surface and the tested compound. The data obtained from theoretical and experimental studies were in reasonable agreement.

Keywords: A9M steel; Corrosion inhibitor; EIS; MD simulation; SEM

Graphical abstract (optional, however strongly recommended)



Specifications Table

Subject area	<i>Organic Chemistry, Computational Chemistry, Chemical Engineering, Corrosion science, Material sciences, Mechanical Engineering Science.</i>
Compounds	<i>Tetramethylammonium hydroxide (TMAH), Industrial water</i>
Data category	<i>Weight loss measurement, polarization curves, X-ray fluorescence spectrometry, electrochemical impedance spectroscopy, Roughness test, Scanning electron microscopy (SEM), Molecular dynamics simulation.</i>
Data acquisition format	Images, data (values) presented in the form of plots and tables
Data type	<i>Raw, analyzed, simulated.</i>
Procedure	<p>Weight loss method <i>Cleaned and pre-weighed coupons of A9M were immersed in industrial water solution with and without different concentrations TMAH. The loss in weight of the steel samples was noted. Corrosion rate was obtained from mass loss measurement of steel sample before and after the addition of inhibitor.</i></p> <p>Electrochemical measurements <i>Both potentiodynamic polarization and electrochemical impedance spectroscopy measurements were performed in a conventional 3-electrode cell with the help of an Autolab (potentiostat / galvanostat) associated with Nova 2 software. A9M steel was used as a working electrode, while platinum and saturated calomel electrodes were used as counter and reference electrodes respectively.</i></p> <p>Surface examination <i>*The general profile of A9M steel surface was characterized by optical microscope after chemical attack with Nital reagent at 3% solution. * The general profile of A9M steel surface roughness before and after treatment with TMAH was recorded. * The surface of A9M steel immersed in IW in the absence and in the presence of TMAH was characterized by Scanning electron microscopy.</i></p>
Data accessibility	<i>All the data have been presented in the paper either in the form of table or plots.</i>

Rationale

The corrosion of metallic surfaces in acidic solutions leads to economic damages in numerous sectors [1]. The use of corrosion inhibitors is mandatory to mitigate the corrosion problems [2-4]. The most well-known corrosion inhibitors are organic compounds, which retard corrosion by adsorbing onto the metal surface by the formation of a coordinate covalent bond or the electrostatic interaction between the metal and inhibitor [5]. Surfactants are substances that modify the surface tension between two surfaces. The surfactants consist of amphiphilic molecules having a lipophilic side (affinity for lipids) and a hydrophilic side (affinity for water). This property also allows them to solubilize two immiscible phases. [6, 7]. The adsorption behavior of surfactants at the metal/solution interface is described by many researchers [8, 9]. In the present work, the effect of the commercial surfactant Tetramethylammonium hydroxide (TMAH) (Fig.1) on the corrosion inhibition of A9M steel in industrial water "IW" by electrochemical impedance spectroscopy (EIS), potentiodynamic polarization, and weight loss measurements methods were studied. In addition, the surface of steel was characterized by optical

microscope, surface roughness and scanning electron microscopy (SEM). Molecular dynamics simulation was used to determine the best adsorption configuration of inhibitor on the metal surface.

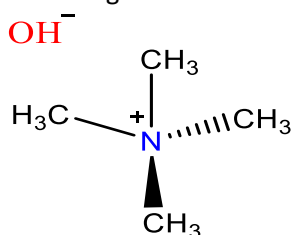


Fig. 1. Molecular structure of tetramethylammonium hydroxide “TMAH”

2. Procedure

2. 1. Materials and sample preparation

The tested inhibitor was Tetramethylammonium hydroxide 25wt. % in H₂O “TMAH” purchased from Sigma-Aldrich incorporated in Fig.1. Cylindrical pieces with a contact area of 5 Cm² and rectangular pieces with (1 cm x 1.5 cm x 0.9 cm) dimension of A9M steel with a purity of 99.54%, (supplied by ARCELORMITTAL – Annaba, ALGERIA) were used as working electrodes for electrochemical and weight loss measurements, respectively. These specimens were pre-treated by grinding with different grades of emery papers from 100 up to 2000, degreased with acetone and rinsed in distilled water before inserting them into the test solution.

The chemical composition of A9M steel obtained by the XRF method (X-ray fluorescence spectrometry) and their mechanical characteristics are given in the Table 1 and Table 2, respectively.

The industrial water obtained from a semi-closed circuit “IW” [pH=6.22, σ (μ .S.m⁻¹)=2.81, TA=8 F°, TAC= 5.8 F°, TH= 9, Cl⁻=49 mg/L, TDS= 245 mg/L, MES= 32 mg/L] was used as corrosive medium. A large range of concentrations, from 0.1 to 0.7% of TMAH, was used for weight loss measurement. Then we chose only three concentrations for electrochemical studies.

Table 1. Weight percent composition of A9M steel used for corrosion tests obtained by the XRF method.

Element	Fe	C	Mn	Si	P	S	Cu	Al	Ti	Nb	Ni	Cr	Mo	V	Sn
wt%	99.54	0.06	0.21	0.02	0.006	0.009	0.030	0.095	0.001	0.001	0.009	0.008	0.003	0.001	0.002

Table 2. Mechanical characteristics of A9M steel (MFL UHP 600 KN equipment).

Elasticity E (MPa)	Resistance R (Mpa)	Lengthening L(%)	Micro Hardness HV	Roughness Ra (μ m)
363.9	500.9	31.6	142.4	2.145

2. 2. Weight loss measurement

Electrochemical experiments were performed using a three-electrode cell: a platinum counter electrode (CE), a saturated calomel electrode (SCE) as a reference electrode and A9M steel as a working electrode (WE). All a tests were carried out under hydrostatic conditions and the temperatures of the solutions during The test was carried out by immersing pretreated and weighted A9M steel specimens in 100 ml of the IW with and without different concentrations of TMAH during 2h, at 298 K. The samples were taken out, rinsed, dried and reweighed using a KERN ALS 220-4N analytical balance (precision \pm 0.1 mg).

2. 3. Electrochemical measurements

Electrochemical measurements were carried out using an Autolab (potentiostat / galvanostat) associated with Nova 2 software. The the experiments were maintained at 298K. Before each measurement, the WE was immersed in the test solution at open circuit potential (OCP) for 60 min to establish steady-state corrosion potential (E_{corr}). After measuring the E_{corr} , the electrochemical measurements were performed:

- The potentiodynamic polarization was carried out in the potential range (-1000 to +1000) mV / SCE with a scan rate of 1 mV/s at 298K.
- The polarization resistance (R_p) was measured from the polarization curves obtained at ± 10 mV with respect to the corrosion potential.
- Electrochemical impedance spectroscopy (EIS) measurements were recorded at open circuit potential from high frequency (HF) (100 KHz) to low frequency (LF) (10 mHz) using a sinusoidal perturbation potential of 10 mV.

2. 5. Surface analysis

2. 5. 1. Optical microscope

For this study, a NICON Eclipse LV150N optical microscope was used to characterize the general profile of the A9M steel surface, after a chemical attack with Nital reagent at a 3% solution for 10 seconds.

2. 5. 2. Roughness test

The general profile of A9M steel surface roughness before and after treatment with TMAH was characterized by MFL UHP 600 KN equipment.

2. 5. 3. Scanning electron microscopy

The surface of A9M steel immersed in IW in the absence and in the presence of TMAH was characterized by scanning electron microscopy of type ZEISS.

2. 6. Molecular dynamics simulation (MD)

The adsorption behavior for TMAH on steel surface has been explored by molecular dynamics (MD) simulation using the Discover module in Materials studio 7.0 (from Accelrys Inc.). The interactions of TMAH molecule and Fe surface were carried out in a simulation box of dimension (24.82×24.82×35.63 Å³) with periodic boundary conditions. The Fe (110) surface was selected to simulate the adsorption process. Three-layered simulation box was built. The first layer was the iron block, the second layer was selected for solution slab, which was constructed by the H₂O and TMAH molecule, and the remaining part was the vacuum layer. After construction of the simulation box, all the bulk atoms of iron were kept "frozen", TMAH and water were allowed to interact with the metal surface freely. Nonbonding, van der Waals and electrostatic interactions were set as atom-based summations using the Ewald summation method with a cutoff radius, spline width, and buffer width were set as 15.5 Å, 1 Å, and 0.5 Å, respectively. The Andersen algorithm [10] was employed to control the temperature of simulation at different levels. The simulation was performed at 298 K, NVT ensemble, with time step of 1 fs and simulation time of 50 ps. The interaction energy $E_{interaction}$ between Fe surface and inhibitor molecule and the binding energy was calculated using the following equations [11]:

$$E_{interaction} = E_{total} - (E_{surface+H_2O} + E_{inhibitor}) \quad (1)$$

$$E_{binding} = -E_{interaction} \quad (2)$$

Where the E_{total} is defined as the total energy of the entire system, $E_{surface+H_2O}$ is defined as the total energy of Fe surface and water molecule and the $E_{inhibitor}$ is the energy of the adsorbed inhibitor molecule on the surface

3. Data, value and validation

3. 1. Weight loss measurement

3. 1. 1. Effect of inhibitor concentrations on the corrosion rate

The influence of the addition of TMAH during 2h at 298 K on the inhibition of A9M steel corrosion in IW medium was studied using weight loss method. The corrosion rate (C_R), the inhibition efficiency IE_w (%) and the surface coverage (θ) were determined by using the following equations [12]:

$$\Delta m = m_1 - m_2 \quad (3)$$

$$C_R = \frac{\Delta m}{At} \quad (4)$$

$$IE_w(\%) = \frac{C_R^0 - C_R}{C_R^0} \times 100 \quad (5)$$

$$\theta = \frac{IE_w\%}{100} \quad (6)$$

Where: m_1 and m_2 are the average weight of specimens (g) before and after immersion, respectively, A is the surface area of A9M steel pieces (cm^2) and t is the exposure time (h). C_R^0 and C_R are the corrosion rate values in the absence and presence of inhibitor, respectively. The inhibition efficiency ($IE_w\%$) and corrosion rate (C_R) values obtained from this method are presented in Table 3. Careful examination of the results showed that in the presence of inhibitor, the rate of corrosion decreases compared with the absence of inhibitor, and the inhibition efficiency increased up on increasing TMAH concentration (till 0.5%). This behavior could be attributed to the increase in adsorption of TMAH at the metal/solution interface on increasing its concentration [13, 14]. An increase of TMAH concentration beyond 0.5% resulted in a diminished corrosion protection. This may be due to the withdrawal of adsorbate (TMAH) back into the bulk solution when the concentration of TMAH closes to or beyond the critical concentration [15]. The above effect leads to the weakening of metal–inhibitor interactions, resulting in the replacement of inhibitor by water with a decrease in inhibition efficiency [16, 17].

Table 3. Weight loss parameters for corrosion of A9M steel in IW in absence and presence of TMAH at 298K

C (%)	C_R ($mg\ cm^{-2}\ h^{-1}$)	$IE_w(\%)$	θ
Blank	0.0464	-	-
0.1	0.0120	78.02	0.7802
0.2	0.0098	78.88	0.7888
0.3	0.0095	79.52	0.7952
0.4	0.0066	85.78	0.8596
0.5	0.0060	86.96	0.8696
0.6	0.0152	67.24	0.6724
0.7	0.0158	65.94	0.6594

3. 1. 2. Effect of temperature and activation parameters

The temperature effect on A9M steel in IW medium in the range 298-328 K, in the presence and absence of optimum concentration of inhibitor during 2 h of immersion, and know more about the change may occur on the metal surface such as rapid etching, desorption of inhibitor molecule [18] were performed using weight loss test. The results are given in Table 4. It is clear from the data in Table 4 that the corrosion rate increases with the rise of temperature and it is more pronounced for an uninhibited solution. We also note that the inhibition efficiency decreased with increased solution temperatures, from 298-328 K, which can be attributed to the decrease of the strength of the adsorption process at high temperature, and can be suggest a physical adsorption type [19].

Table 4. Weight loss parameters for corrosion of A9M steel in IW medium in absence and presence 0.5% of TMAH at different temperatures.

T(K)	Blank	TMAH	IE _w (%)
	C _R (mg cm ⁻² h ⁻¹)	C _R (mg cm ⁻² h ⁻¹)	
298	0.0464	0.0060	86.96
303	0.0670	0.0098	85.37
318	0.1148	0.0214	81.36
328	0.1550	0.0344	77.80

In order to determine the activation parameters of the corrosion process, Arrhenius and transition state equations were used [20] :

$$C_R = A \exp\left(\frac{-E_a}{RT}\right) \quad (7)$$

$$C_R = \frac{RT}{Nh} \exp\left(-\frac{\Delta H_a^0}{RT}\right) \exp\frac{\Delta S_a^0}{R} \quad (8)$$

where E_a is the apparent activation energy, A is the Arrhenius pre-exponential, and h is the Plank's constant, N is the Avogadro's number, ΔS_a^0 is the entropy of activation and ΔH_a^0 is the enthalpy of activation. All values of E_a , ΔH_a^0 and ΔS_a^0 were calculated from the slopes and intercepts of the plots: $\ln C_R$ and $\ln (C_R/T)$ versus $1/T$ (Fig. 2 (a), (b)) and listed in Table 5. The E_a value in the presence of 0.5 % of TMAH is higher compared in their absence. This behavior may be attributed to a physical adsorption [21]. On the other hand, the positive values of the enthalpy reflect the endothermic nature of the corrosion process, and the increase in ΔS_a^0 in the presence of TMAH implies an increase in disorder which took place on going from reactants to the metal/solution interface [22].

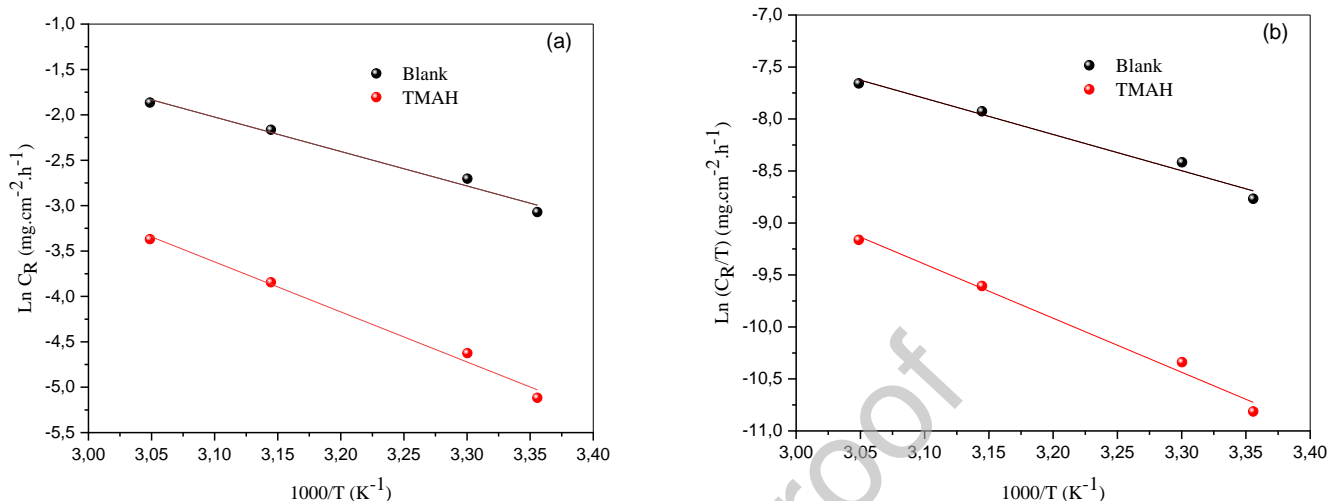


Fig. 2. (a) Arrhenius and (b) transition state plots for A9M steel with and without 0.5% of TMAH.

Table 5. Corrosion kinetic parameters for A9M steel in 1W in absence and presence of 0.5% of TMAH.

Inhibitor	E_a (KJ.mol ⁻¹)	ΔH_a^0 (KJ.mol ⁻¹)	ΔS_a^0 (J.mol ⁻¹ .K ⁻¹)
Blank	31.56	28.96	-134.33
TMAH	45.81	43.22	-103.38

3. 2. Adsorption isotherm

In order to understand the corrosion adsorption processes that occur onto the steel surface, the adsorption isotherm was calculated. Several isotherms such as Langmuir, Frumkin and Temkin models were applied in order to explain the adsorption process of TMAH on the A9M steel surface. In our present study, the Langmuir isotherm was found to fit well with experimental data obtained with correlation coefficient value ($R^2=0.996$), and they are given by the following equation [23]:

$$\frac{C}{\theta} = \frac{1}{K_{ads}} + C \quad (9)$$

where C is the inhibitor concentration, θ is the surface coverage and K_{ads} is the adsorption equilibrium constant. Fig. 3. showed the plots of C/θ versus C for TMAH at 298 K. The equilibrium adsorption constant K_{ads} is related to the standard Gibbs free energy of adsorption ΔG_{ads}^0 as follow [24]:

$$\Delta G_{ads}^0 = -RT \ln (55.5 \cdot K_{ads}) \quad (10)$$

Where 55.5 is the concentration of water in solution (mol/L), R is the gas constant and T is the absolute temperature (K). The higher negative values of ΔG_{ads}^0 (-19.67 KJ/mol) indicate that the inhibitor

molecules adsorbed strongly and spontaneously on the metal surface, and their value is around -20 KJ/mol, this signifies that the adsorption of TMAH on the steel surface involves physical adsorption [24].

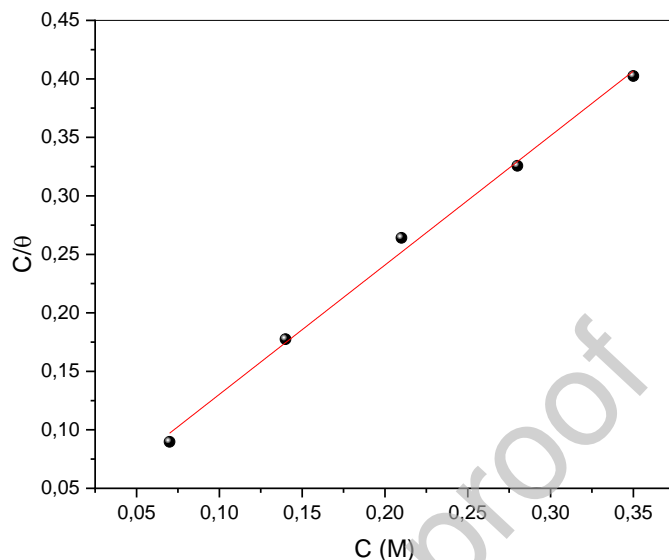


Fig. 3. Langmuir adsorption isotherm models for adsorption of inhibitor on A9M steel, at 298 K.

3. 3. Electrochemical Measurements

3. 3. 1. Potentiodynamic polarization curves

The effect of the addition of TMAH on the anodic and cathodic polarization curves of A9M steel in the IW medium at 298 K is shown in Fig. 4. The corrosion kinetic parameters such as corrosion current density (i_{corr}), corrosion potential (E_{corr}), the anodic Tafel slopes (β_a), cathodic Tafel slope (β_c), and the inhibition efficiency ($IE_p(\%)$) for A9M steel in IW solution in the absence and presence of different concentrations of TMAH are listed in Table 6. The values of $IE_p(\%)$ are calculated using the following equation:

$$IE_p(\%) = \frac{i_{corr} - i'_{corr}}{i_{corr}} \times 100 \quad (11)$$

Where: i_{corr} and i'_{corr} represent the corrosion current density values of A9M steel in the absence and presence of inhibitor, respectively.

According to the polarization curves, the increase in the TMAH concentration displaces the corrosion potential towards the anode domain and shifted both cathodic and anodic branches to lower current densities, which suggest that the inhibitor molecule suppressed the anodic dissolution and subsequent reduction of hydrogen evolution reaction [24, 25]. It is reported in the literature that, if the displacement in $E_{corr} > 85$ mV, the inhibitor acts as cathodic or anodic inhibitor; the inhibitor classified as a mixed type inhibitor if $E_{corr} < 85$ mV [26]. By inspecting the results in Table 6, the values of β_c change markedly in the presence of inhibitor molecule and the shift of E_{corr} value compared to the blank were more than 85 mV, which suggested that our inhibitor act as cathodic inhibitor. Furthermore, the current

density of corrosion (i_{corr}) values decreased with increasing the concentration of TMAH, and reached a value of $35.62 \times 10^{-7} \text{ A/cm}^2$, at the optimum concentration of inhibitor 0.5%, which led to a maximum value of $IE_p\%$ (91.22%). Suggesting that the inhibitor molecule was adsorbed on the surface of A9M steel to form a protective film which reduces the active sites exposed on the surface of the steel [27].

Table 6. Polarization parameters and the inhibition efficiency of A9M steel corrosion in IW medium containing different concentrations of TMAH at 298 K.

C (%)	$-E_{corr}$ (mV/SCE)	i_{corr} (A/cm^2)	β_a (mV.dec^{-1})	$-\beta_c$ (mV.dec^{-1})	R_p ($\Omega.\text{cm}^2$)	IE_p (%)
0	589	159.62×10^{-7}	0.214	0.137	1.388×10^5	/
0.3	376	22.74×10^{-7}	0.161	0.512	1.423×10^5	85.75
0.5	392	14.00×10^{-7}	0.200	0.868	1.769×10^5	91.22
0.7	407	35.62×10^{-7}	0.187	0.804	1.824×10^5	77.68

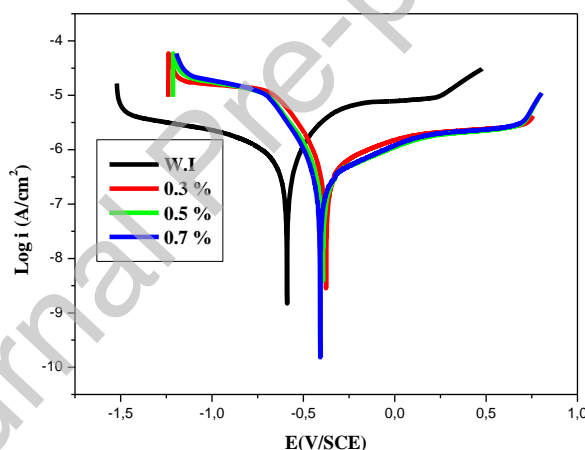


Fig. 4. Potentiodynamic polarization curves of A9M steel in IW solution, in the presence and absence of different TMAH concentrations at 298 K.

3.3.2. EIS analysis

For more information about the corrosion inhibitor performance, and to study the corrosion mechanism, electrochemical impedance spectroscopy was done. The EIS curves (Nyquist and bode plots) for A9M steel with different concentrations of TMAH in the IW solution are shown in Fig. 5a, b, and c. As shown in this Figure, we remark that when TMAH is added to the industrial water, the size of the impedance diagram increases with the increasing ϕ concentration and consequently the inhibitory efficacy increases, due to the adsorption of inhibitor molecules on the steel surface [28]. Examination of Fig. 5a reveals that each impedance diagram in the presence and the absence of TMAH at different concentration consists of a single capacitive loop at high frequency (HF) with one capacitive time

constant in the Bode plots on the same Fig 5 b. The capacitive loop indicates that, the corrosion process has been controlled by a single phenomenon, which is charge transfer [29]. While those according to the module (Fig. 5 c) show that the polarization resistance increases as the concentration of TMAH increases up to 0.5%. The impedance diagrams obtained are not perfect semicircles, this may be attributed to the frequency dispersion effect resulting from the roughness and inhomogeneity of the surface of A9M steel [30]. Therefore, a constant phase element (CPE) was used to replace of the capacity of the double layer C_{dl} to get a more precise fit of experimental data and the impedance is given by Eq. (12) [3]:

$$Z_{CPE} = \frac{1}{Q(j\omega)^\alpha} \quad (12)$$

Where: Q ($\Omega^{-1}.s^\alpha .cm^{-2}$) is the magnitude of the CPE; j is the imaginary number ($j^2 = -1$); ω is the angular frequency; α is the deviation parameter ($-1 \leq \alpha \leq 1$) it characterizes the properties of CPE [31, 32]. The equivalent circuit describing the electrochemical behavior of the A9M/ IW interface in the absence and in the presence of TMAH is shown in Fig. 6.

Fig. 7 shows the fitting of impedance data. The coefficient of adequacy (χ^2) value as obtained by the fitting of impedance data on the corresponding data for the equivalent circuit is found to be 32×10^{-3} for 0.5% of TMAH, which confirms the model presented in Fig. 6.

Several parameters for the impedance spectra are denoted in Table 5. The inhibition efficiency ($IE_R\%$) from the charge transfer resistance was calculated according to the following equation [33]:

$$IE_R (\%) = \frac{R_{ct}' - R_{ct}}{R_{ct}'} \times 100 \quad (13)$$

Where: R_{ct} and R_{ct}' represents the resistance of charge transfer in the absence and in the presence of the inhibitor, respectively.

The data presented in Table 7 show that the R_{ct} value increases with the addition of inhibitor compared to in their absence, could be attributed to the formation of a protective film at metal / solution interface that can reduce the transfer of electrons between the metal surface and the corrosive medium, which increases the effectiveness of the protection [27, 34]. Therefore, good inhibition efficiency was observed (91.65%). The results obtained by the EIS study correlate very well with the potentiodynamic results. The inhibition efficiencies show a good quantitative correlation.

Table 7. Impedance parameters and inhibition efficiency values for A9M in IW containing different concentrations of TMAH at 298 K.

C (%)	R_e ($\Omega.cm^2$)	CPE_{dl} ($F.s^{1/n}$)	n	R_{ct} ($\Omega.cm^2$)	E (%)
0	67.2	$10.59 \cdot 10^{-6}$	0.7	105849.56	/
0.3	66.2	$11.0 \cdot 10^{-6}$	0.8	14682.08	86.12
0.5	68.7	$8.12 \cdot 10^{-6}$	0.9	8833.79	91.65
0.7	65.4	$13.4 \cdot 10^{-6}$	0.8	23407.63	77.88

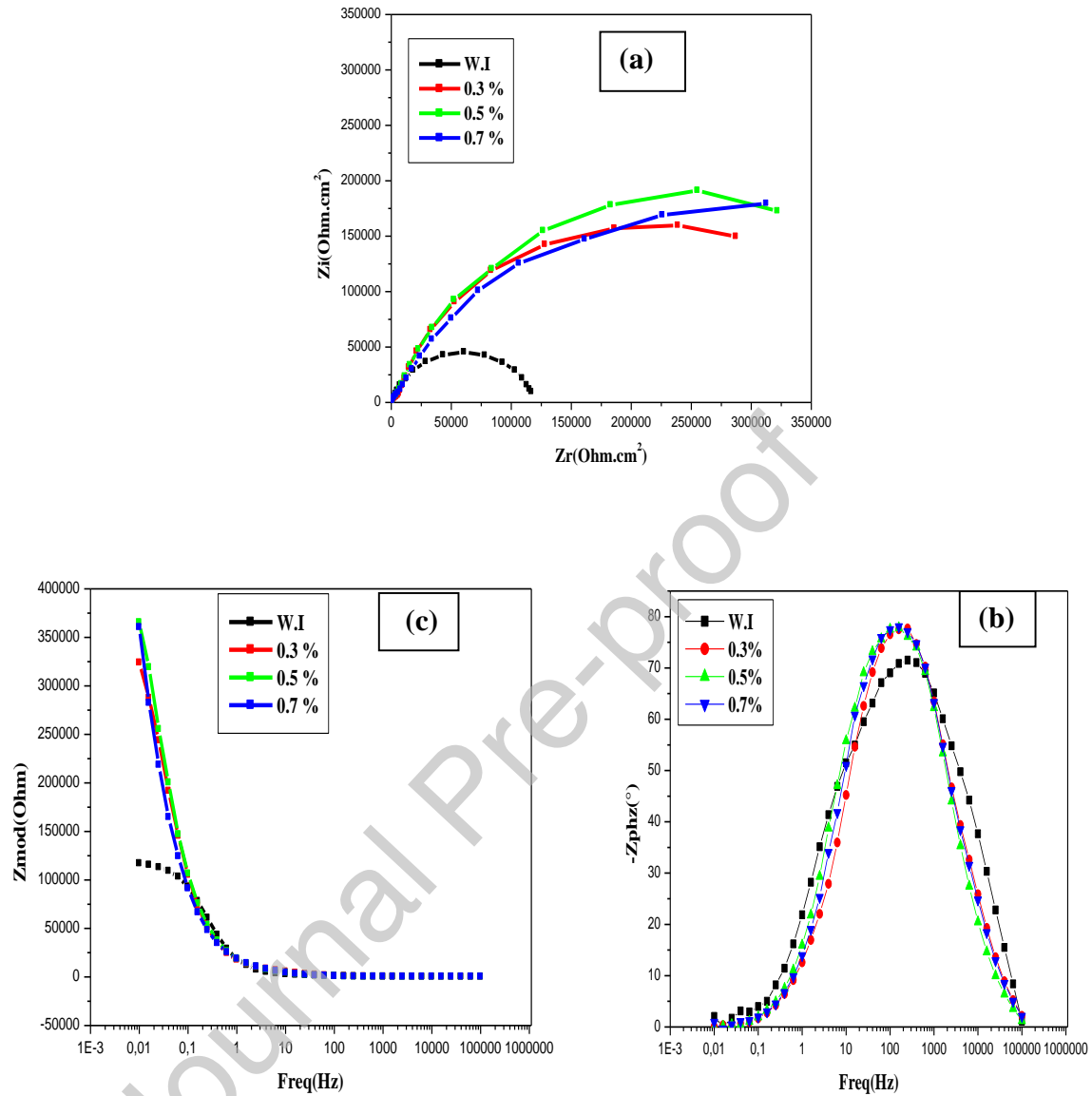


Fig. 5. Nyquist (a) and Bode (b and c) plots for A9M steel in IW solution in the absence and in the presence of different concentrations of TMAH at 298

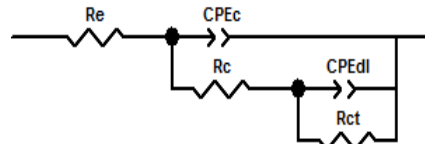


Fig. 6. Equivalent circuit used for modelling the interface A9M steel / IW solution without and with TMAH.

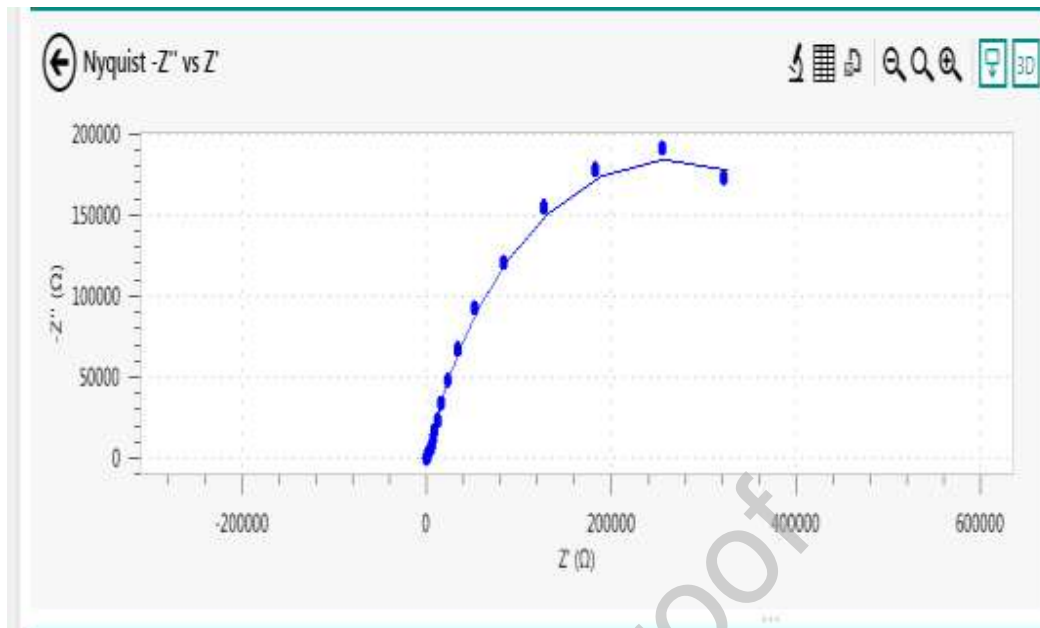


Fig. 7. Nyquist fitting of experimental data of A9M in 1W in the presence of 0.5% M of TMAH.

3. 4. Surface analysis

3. 4. 1. Roughness test

The general profile of A9M steel surface roughness before and after treatment with TMAH was represented in Fig 8a and 8b, respectively. The Figure showed a decrease in surface roughness for the treated specimens with TMAH. A9M steel without immersion in a solution indicates the level of surface roughness value to be $2.145 \mu\text{m}$. While the surface roughness of the A9M steel sample treated with TMAH solution shows the decrease of the surface roughness rate to $0.021 \mu\text{m}$, which indicates the formation of a protective film.

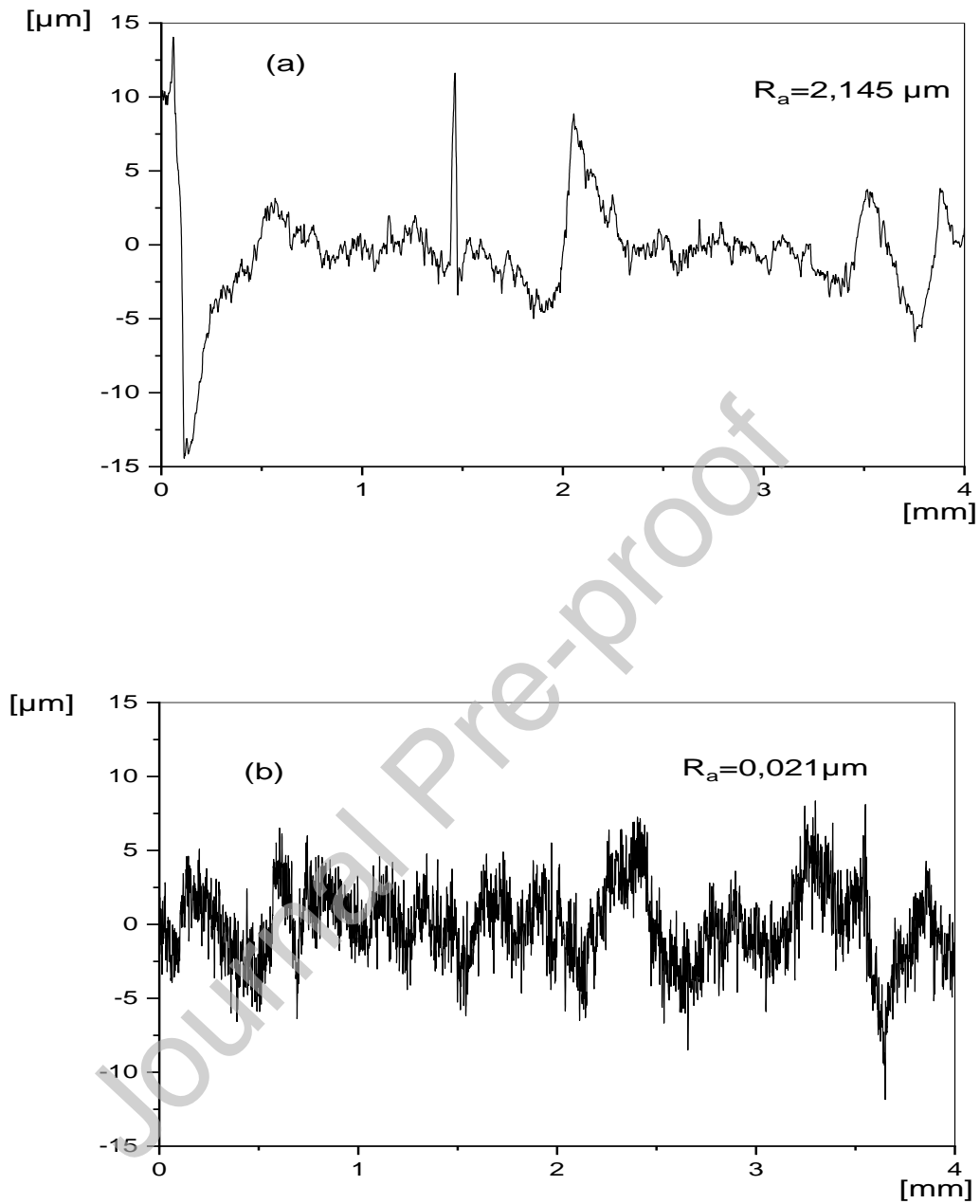


Fig. 8. General surface profile of A9M steel (a) before treatment, (b) after treatment with 0.5% TMAH.

3. 4. 2. Structural characterization by Optical microscope

Optical microscope observations were mainly used to characterize the microstructure of A9M steel and help us understand the phenomena occurring at the metal/solution interface. The microstructure of the A9M steel is shown in Fig. 9. The following metallographs (via Fig. 9) show a fine structure of ferrite and perlite of A9M steel of micro-hardness 142.4 HV_{0.2}. The dark ranges correspond to the perlite while the clear ones correspond to the ferrite.

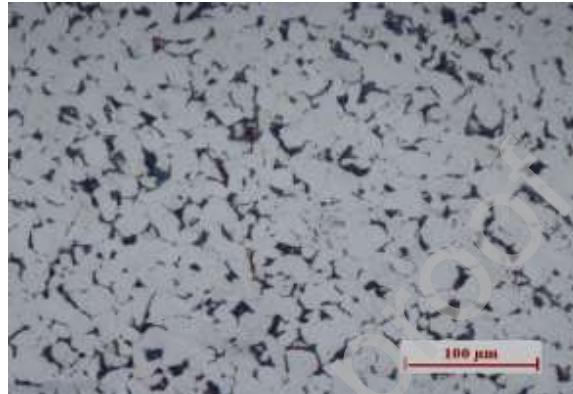


Fig. 9. Optical micrographs of A9M steel

3. 4. 5. Analysis by scanning electron microscopy (SEM)

Fig. 10 depicted the micrographs obtained after 2 h of immersion at 298 K in industrial water in the absence and presence of 0.5% TMAH. In Fig. 10a, we observe that the immersed steel surface in industrial water for 2h suffers severe damage due to corrosive attack. On the other hand, with the addition of the optimum concentration of TMAH (Fig. 10b), we observe that the steel surface damage considerably decreased in which an almost smooth surface can be seen, indicating that the surface is covered by a protective film. We can conclude that TMAH protects A9M steel from corrosion by the formation of protective layer (film).

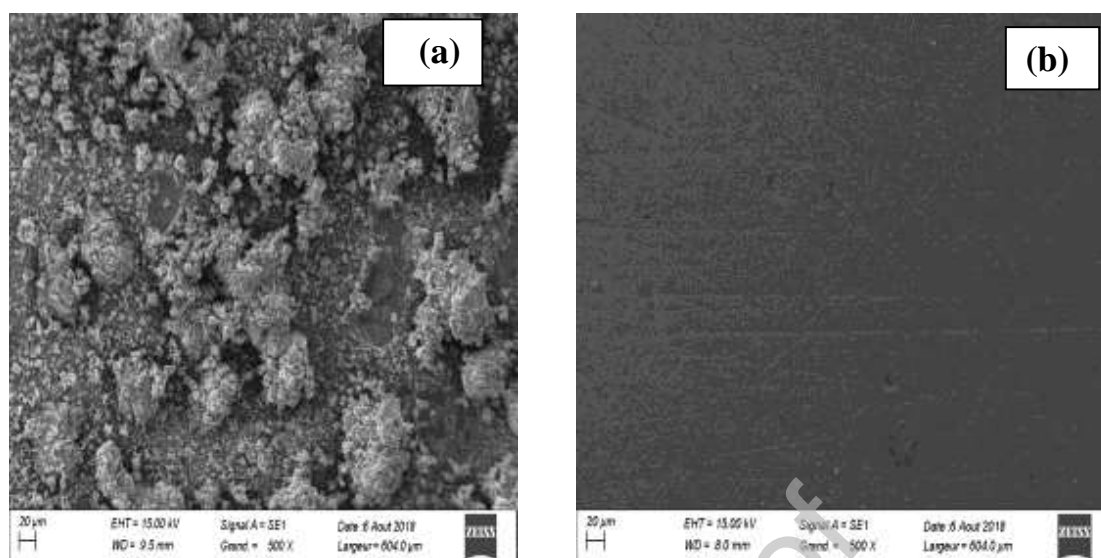


Fig. 10. SEM micrographs of A9M steel surfaces (a) without inhibitor, (b) with inhibitor immersed in industrial water solution for 2h at 298K.

3. 5. Molecular dynamics simulation

Recently, several groups of researchers have employed MD simulations to explore the mechanism of adsorption of the inhibitor molecules on the surface atoms of the metals [35-38]. The simulation reached its equilibrium state when the temperature and energy fluctuation of the system attained the steady state [39]. As can be seen from Fig. 11 that both energy and temperature reach the balance, which indicates that, the whole system has reached equilibrium. Fig. 12 shows the equilibrium adsorption configurations of the most stable adsorption of TMAH on Fe (1 1 0) surface. It clearly observed from Fig.12, that the TMAH molecule was adsorbed nearly to Fe surface. The obtained $E_{\text{interaction}}$ and E_{binding} values are tabulated in Table 8. The obtained value of interaction energy is negative and it suggests spontaneous, strong and stable adsorption of inhibitor molecules on the Fe (1 1 0) surfaces [35].

- Pair correlation function

The pair correlation function was computed from MD simulations and it is used as a useful method to calculate the bond length between molecule atoms and metal surface to estimate the interaction types [40]. The typical length for chemical bond is 1–3.5 Å, while that of the Coulomb and van der Waals forces is longer than 3.5 Å [29]. From Fig. 13, the distance between Fe-N (3.63 Å), Fe-O (4.56 Å) and Fe-C (4.74 Å) are more than 3.5 Å, suggesting the presence of Vander Walls and/or coulomb interaction (physisorption) between these atoms and iron atoms.

Table 8. Interaction energies between the inhibitor and Fe (110) surface in aqueous phase (kJ/mol).

System	Binding energy	Interaction energy
Fe (1 1 0)+TMAH	924,285	-924,285

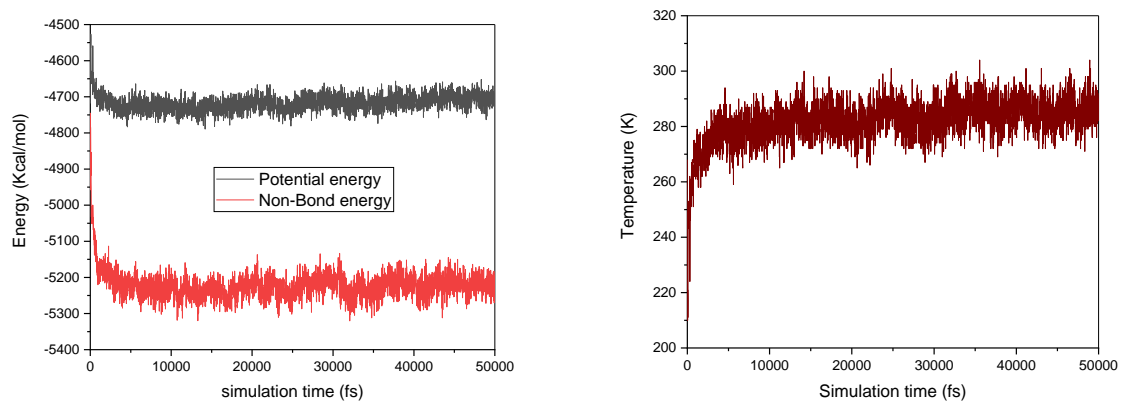


Fig. 11. Energy and temperature equilibrium curves obtained using MD simulation for TMAH molecule.

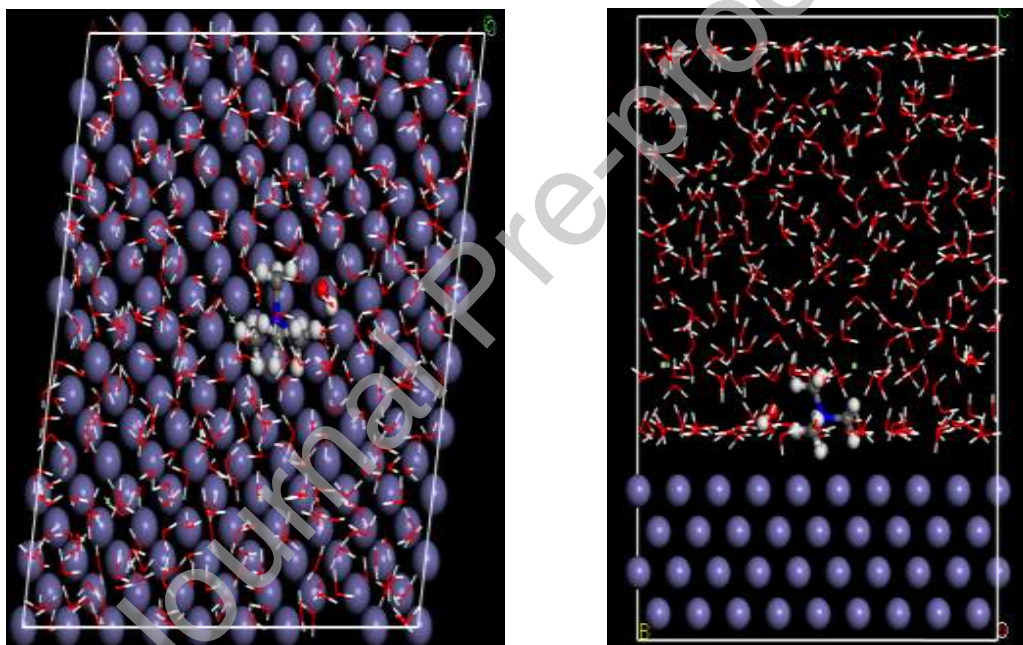


Fig. 12. Equilibrium adsorption configurations of TMAH on Fe (1 1 0) surface in water solution (top and side view)

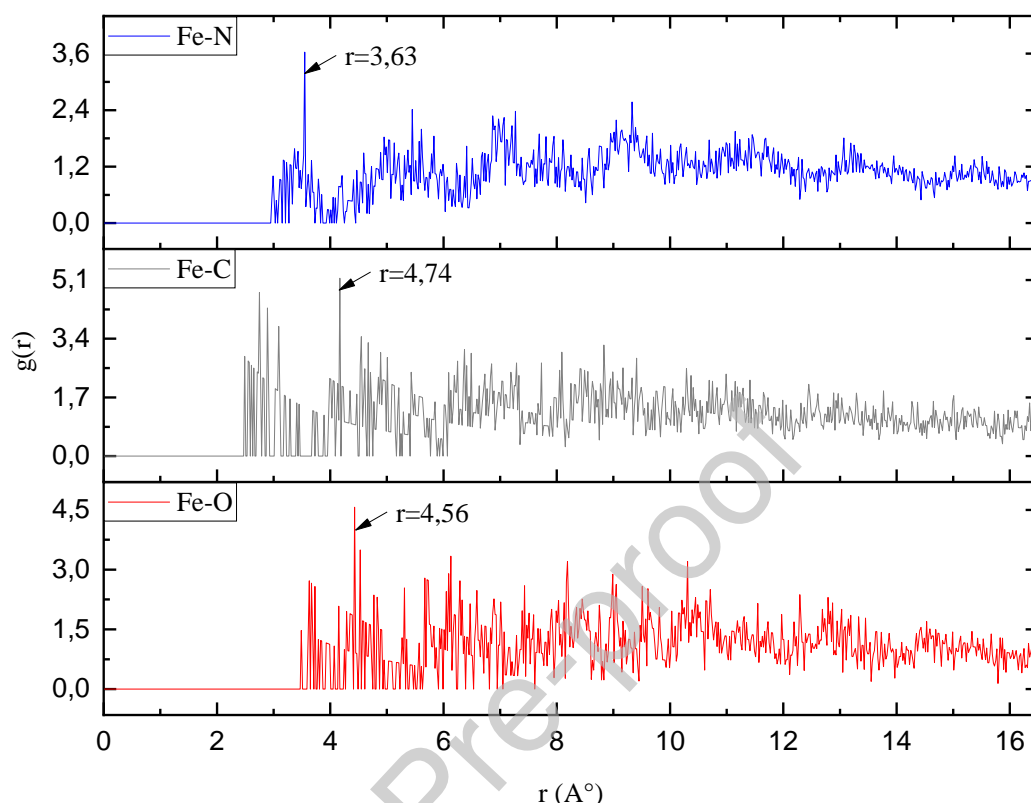


Fig .13. Pair correlation function of N, O, C atoms from TMAH molecule with Fe (110) surface in aqueous solution.

4. Conclusion

From the results obtained, the following conclusions could be drawn

- TMAH was found to inhibit the corrosion of A9M steel in industrial water medium.
- Potentiodynamic polarization results suggest that TMAH compound acts as anodic type corrosion inhibitor.
- The EIS results indicate that, the presence of TMAH in industrial water increases the value of R_{ct} and reduces the value of C_{dl} . Whereas the EIS spectra reveals one capacitive loop which suggests that the corrosion of AA9M steel is controlled by charge transfer process.
- Roughness test and SEM methods confirmed the formation of inhibitor film.
- The negative value of interaction energy in MD indicates the strong and spontaneous interaction between metal and inhibitor molecules.

Conflict of interest

On behalf of all authors, the corresponding author states that there is no conflict of interest.

References

- [1] A. Fouda, S.A. El-Maksoud, A. Belal, A. El-Hossiany, A. Ibrahim, Effectiveness of Some Organic Compounds as Corrosion Inhibitors for Stainless Steel 201 in 1M HCl: Experimental and Theoretical Studies, *Int. J. Electrochem. Sci*, 13 (2018) 9826-9846.
- [2] H.-L. Wang, R.-B. Liu, J. Xin, Inhibiting effects of some mercapto-triazole derivatives on the corrosion of mild steel in 1.0 M HCl medium, *Corros. Sci*, 46 (2004) 2455-2466.
- [3] H. Ouici, M. Tourabi, O. Benali, C. Selles, C. Jama, A. Zarrouk, F. Bentiss, Adsorption and corrosion inhibition properties of 5-amino 1, 3, 4-thiadiazole-2-thiol on the mild steel in hydrochloric acid medium: Thermodynamic, surface and electrochemical studies, *J. Electroanalytical. Chem*, 803 (2017) 125-134.
- [4] N.J. Nnaji, O.T. Ujam, N.E. Ibisi, J.U. Ani, T.O. Onuegbu, L.O. Olasunkanmi, E.E. Ebenso, Morpholine and piperazine based carboxamide derivatives as corrosion inhibitors of mild steel in HCl medium, *J. Mol. Liq*, 230 (2017) 652-661.
- [5] D.B. Hmamou, R. Salghi, A. Zarrouk, H. Zarrok, R. Touzani, B. Hammouti, A. El Assyry, Investigation of corrosion inhibition of carbon steel in 0.5 M H₂SO₄ by new bipyrazole derivative using experimental and theoretical approaches, *J. Envir. Chem. Eng*, 3 (2015) 2031-2041.
- [6] A. Badawi, M. Hegazy, A. El-Sawy, H. Ahmed, W. Kamel, Novel quaternary ammonium hydroxide cationic surfactants as corrosion inhibitors for carbon steel and as biocides for sulfate reducing bacteria (SRB), *Mater. Chem. Phys*, 124 (2010) 458-465.
- [7] N. Negm, A. Al Sabagh, M. Migahed, H.A. Bary, H. El Din, Effectiveness of some diquaternary ammonium surfactants as corrosion inhibitors for carbon steel in 0.5 M HCl solution, *Corros. Sci*, 52 (2010) 2122-2132.
- [8] H. Luo, Y. Guan, K. Han, Inhibition of mild steel corrosion by sodium dodecyl benzene sulfonate and sodium oleate in acidic solutions, *Corrosion*, 54 (1998) 619-627.
- [9] C.J. van Oss, *Interfacial Phenomena in Apolar Media (Surfactant Science Series Vol. 21)*. HF Eicke and GD Parfitt, eds. Marcel Dekker, Inc., New York and Basel, 1987, pp ix+ 416, \$99.75, *JOURNAL OF DISPERSION SCIENCE AND TECHNOLOGY*, 11 (1990) 435-436.
- [10] H.C. Andersen, Molecular dynamics simulations at constant pressure and/or temperature, *The Journal of chemical physics*, 72 (1980) 2384-2393.
- [11] Z. Zhang, N. Tian, X. Huang, W. Shang, L. Wu, Synergistic inhibition of carbon steel corrosion in 0.5 M HCl solution by indigo carmine and some cationic organic compounds: experimental and theoretical studies, *RSC Advances*, 6 (2016) 22250-22268.
- [12] M.N. El-Haddad, A. Fouda, A. Hassan, Data from Chemical, electrochemical and quantum chemical studies for interaction between Cephapirin drug as an eco-friendly corrosion inhibitor and carbon steel surface in acidic medium, *Chemical Data Collections*, 22 (2019) 100251.
- [13] M. El Faydy, M. Galai, A. El Assyry, A. Tazouti, R. Touir, B. Lakhrissi, M.E. Touhami, A. Zarrouk, Experimental investigation on the corrosion inhibition of carbon steel by 5-(chloromethyl)-8-quinolinol hydrochloride in hydrochloric acid solution, *Journal of Molecular Liquids*, 219 (2016) 396-404.
- [14] A. Oulabbas, S. Abderrahmane, Natural extract of *Opuntia ficus indica* as green inhibitor for corrosion of XC52 steel in 1 M H₃PO₄, *Materials Research Express*, 6 (2018) 015513.
- [15] A. Satapathy, G. Gunasekaran, S. Sahoo, K. Amit, P. Rodrigues, Corrosion inhibition by *Justicia gendarussa* plant extract in hydrochloric acid solution, *Corrosion science*, 51 (2009) 2848-2856.
- [16] G. Gunasekaran, L. Chauhan, Eco friendly inhibitor for corrosion inhibition of mild steel in phosphoric acid medium, *Electrochimica acta*, 49 (2004) 4387-4395.
- [17] M.H. Hussin, M.J. Kassim, The corrosion inhibition and adsorption behavior of *Uncaria gambir* extract on mild steel in 1 M HCl, *Materials Chemistry and Physics*, 125 (2011) 461-468.
- [18] A. Chaouikia, H. Lgaza, R. Salghib, S.L. Gaonkarc, K.S. Bhatc, S. Jodehd, K. Toumiate, H. Ouddaa, New Benzohydrazide Derivative as Corrosion Inhibitor for Carbon Steel in a 1.0 M HCl Solution:

- Electrochemical, DFT and Monte Carlo Simulation Studies, *Portugaliae Electrochimica Acta*, 37 (2019) 147-165.
- [19] H. Zarrok, A. Zarrouk, B. Hammouti, R. Salghi, C. Jama, F. Bentiss, Corrosion control of carbon steel in phosphoric acid by purpald–weight loss, electrochemical and XPS studies, *Corrosion Science*, 64 (2012) 243-252.
- [20] M. Behpour, S. Ghoreishi, N. Soltani, M. Salavati-Niasari, The inhibitive effect of some bis-N, S-bidentate Schiff bases on corrosion behaviour of 304 stainless steel in hydrochloric acid solution, *Corrosion Science*, 51 (2009) 1073-1082.
- [21] R. Solmaz, Investigation of adsorption and corrosion inhibition of mild steel in hydrochloric acid solution by 5-(4-Dimethylaminobenzylidene) rhodanine, *Corrosion Science*, 79 (2014) 169-176.
- [22] B. Xu, W. Gong, K. Zhang, W. Yang, Y. Liu, X. Yin, H. Shi, Y. Chen, Theoretical prediction and experimental study of 1-butyl-2-(4-methylphenyl) benzimidazole as a novel corrosion inhibitor for mild steel in hydrochloric acid, *Journal of the Taiwan Institute of Chemical Engineers*, 51 (2015) 193-200.
- [23] M. Benahmed, I. Selatnia, N. Djeddi, S. Akkal, H. Laouer, Adsorption and Corrosion Inhibition Properties of Butanolic Extract of *Elaeoselinum thapsioides* and Its Synergistic Effect with *Reutera lutea* (Desf.) Maires (Apiaceae) on A283 carbon Steel in Hydrochloric Acid Solution, *Chemistry Africa*, (2019) 1-11.
- [24] I. Selatnia, A. Sid, M. Benahmed, T. Ozturk, N. Gherraf, Synthesis and Characterization of a Bis-Pyrazoline Derivative as Corrosion Inhibitor for A283 Carbon Steel in 1M HCl: Electrochemical, Surface, DFT and MD Simulation Studies, *Protection of Metals and Physical Chemistry of Surfaces*, 54 (2018) 1182-1193.
- [25] Z. Rouifi, F. Benhiba, M. El Faydy, T. Laabiassi, H. About, H. Oudda, I. Warad, A. Guenbour, B. Lakhrissi, A. Zarrouk, Performance and computational studies of new soluble triazole as corrosion inhibitor for carbon steel in HCl, *Chemical Data Collections*, (2019) 100242.
- [26] N. Djeddi, M. Benahmed, S. Akkal, H. Laouer, E. Makhloufi, N. Gherraf, Study on methylene dichloride and butanolic extracts of *Reutera lutea* (Desf.) Maire (Apiaceae) as effective corrosion inhibitions for carbon steel in HCl solution, *Research on Chemical Intermediates*, 41 (2015) 4595-4616.
- [27] M. Yadav, S. Kumar, T. Purkait, L. Olasunkanmi, I. Bahadur, E. Ebenso, Electrochemical, thermodynamic and quantum chemical studies of synthesized benzimidazole derivatives as corrosion inhibitors for N80 steel in hydrochloric acid, *Journal of Molecular Liquids*, 213 (2016) 122-138.
- [28] R. Solmaz, Investigation of the inhibition effect of 5-((E)-4-phenylbuta-1, 3-dienylideneamino)-1, 3, 4-thiadiazole-2-thiol Schiff base on mild steel corrosion in hydrochloric acid, *Corrosion Science*, 52 (2010) 3321-3330.
- [29] K. Abderrahim, I. Selatnia, A. Sid, P. Mosset, 1, 2-bis (4-chlorobenzylidene) Azine as new and effective corrosion inhibitor for copper in 0.1 N HCl: A combined experimental and theoretical approach, *Chemical Physics Letters*, 707 (2018) 117-128.
- [30] B. Xu, Y. Ji, X. Zhang, X. Jin, W. Yang, Y. Chen, Experimental and theoretical evaluation of N, N-Bis (2-pyridylmethyl) aniline as a novel corrosion inhibitor for mild steel in hydrochloric acid, *Journal of the Taiwan Institute of Chemical Engineers*, 59 (2016) 526-535.
- [31] S. RameshKumar, I. Danaee, M. RashvandAvei, M. Vijayan, Quantum chemical and experimental investigations on equipotent effects of (+) R and (–) S enantiomers of racemic amisulpride as eco-friendly corrosion inhibitors for mild steel in acidic solution, *Journal of Molecular Liquids*, 212 (2015) 168-186.
- [32] N. Yilmaz, A. Fitoz, K.C. Emregül, A combined electrochemical and theoretical study into the effect of 2-((thiazole-2-ylimino) methyl) phenol as a corrosion inhibitor for mild steel in a highly acidic environment, *Corrosion Science*, 111 (2016) 110-120.

- [33] P.B. Raja, A.A. Rahim, H. Osman, K. Awang, Inhibitive effect of *Xylopi*a ferruginea extract on the corrosion of mild steel in 1M HCl medium, *International Journal of Minerals, Metallurgy, and Materials*, 18 (2011) 413.
- [34] M. Shabani-Nooshabadi, M. Ghandchi, *Santolina chamaecyparissus* extract as a natural source inhibitor for 304 stainless steel corrosion in 3.5% NaCl, *Journal of Industrial and Engineering Chemistry*, 31 (2015) 231-237.
- [35] H. Mi, G. Xiao, X. Chen, Theoretical evaluation of corrosion inhibition performance of three antipyrine compounds, *Computational and Theoretical Chemistry*, 1072 (2015) 7-14.
- [36] S. Kaya, C. Kaya, L. Guo, F. Kandemirli, B. Tüzün, İ. Uğurlu, L.H. Madkour, M. Saraçoğlu, Quantum chemical and molecular dynamics simulation studies on inhibition performances of some thiazole and thiadiazole derivatives against corrosion of iron, *Journal of Molecular Liquids*, 219 (2016) 497-504.
- [37] L.H. Madkour, S. Kaya, C. Kaya, L. Guo, Quantum chemical calculations, molecular dynamics simulation and experimental studies of using some azo dyes as corrosion inhibitors for iron. Part 1: Mono-azo dye derivatives, *Journal of the Taiwan Institute of Chemical Engineers*, 68 (2016) 461-480.
- [38] M. Shahraki, M. Dehdab, S. Elmi, Theoretical studies on the corrosion inhibition performance of three amine derivatives on carbon steel: molecular dynamics simulation and density functional theory approaches, *Journal of the Taiwan Institute of Chemical Engineers*, 62 (2016) 313-321.
- [39] S.K. Saha, M. Murmu, N.C. Murmu, I. Obot, P. Banerjee, Molecular level insights for the corrosion inhibition effectiveness of three amine derivatives on the carbon steel surface in the adverse medium: A combined density functional theory and molecular dynamics simulation study, *Surfaces and Interfaces*, 10 (2018) 65-73.
- [40] H. Lgaz, S.K. Saha, A. Chaouiki, K.S. Bhat, R. Salghi, P. Banerjee, I.H. Ali, M.I. Khan, I.-M. Chung, Exploring the potential role of pyrazoline derivatives in corrosion inhibition of mild steel in hydrochloric acid solution: Insights from experimental and computational studies, *Construction and Building Materials*, 233 (2020) 117320.